



**Forschungszentrum Karlsruhe**  
Technik und Umwelt

**Wissenschaftliche Berichte**  
FZKA 5565

**Studies of Continuum  
Coupling Effects in  
 ${}^6\text{Li}$  ( $\alpha, \alpha'$ ) and  
 ${}^6\text{Li}$  ( $p, p'$ ) Excitation**

**R. Kanungo, M. Lahiri, C. Samanta, H. Rebel**  
Institut für Kernphysik

Mai 1995

---



**FORSCHUNGSZENTRUM KARLSRUHE**  
**Technik und Umwelt**

**Wissenschaftliche Berichte**  
**FZKA 5565**

**Studies of Continuum Coupling Effects**  
**in  ${}^6\text{Li}$  ( $\alpha, \alpha'$ ) and  ${}^6\text{Li}$  ( $p, p'$ ) Excitation**

**Rituparna Kanungo\*, Manideepa Lahiri\*, Chhanda Samanta\***  
**and Heinigerd Rebel**

**Institut für Kernphysik**

**\* Saha Institute of Nuclear Physics, Calcutta**

**Forschungszentrum Karlsruhe GmbH, Karlsruhe**

**1995**

Als Manuskript gedruckt  
Für diesen Bericht behalten wir uns alle Rechte vor

Forschungszentrum Karlsruhe GmbH  
Postfach 3640, 76021 Karlsruhe

ISSN 0947-8620

## Abstract

The nonresonant continuum part of  ${}^6\text{Li} \Rightarrow \alpha + d$  breakup at low relative fragment energies, induced by 50-MeV  $\alpha$ -particle and 65-MeV proton scattering, is discretized in two separate energy bins. Realistic coupled-channel analyses are carried out, coupling the  $1^+$  ground state with both the resonant  $3_1^+$  state as well as the two nonresonant discretized continuum states, including selfcoupling. A simultaneous fit to the data puts stringent constraints on the coupling strengths. It delineates that their arbitrary variation is unacceptable and that the complex coupling schemes in CDCC calculations need sufficient experimental control. The coupling effects by multistep processes (virtual excitations) through intermediate continuum states prove to be marginal in the considered  ${}^6\text{Li}(\alpha, \alpha'){}^6\text{Li}^*$  and  ${}^6\text{Li}(p, p'){}^6\text{Li}^*$  cases.

## Untersuchung von Kontinuum-Kopplungseffekten in ${}^6\text{Li}(\alpha, \alpha')$ und ${}^6\text{Li}(p, p')$ -Anregungen

Das nichtresonante Kontinuum des  ${}^6\text{Li} \Rightarrow \alpha + d$  Aufbruchs bei niedrigen Relativenergien der Fragmente, angeregt durch 50-MeV Alphateilchen und 65-MeV Proton-Streuung, wird in zwei getrennte Energie-Bins diskretisiert. Es werden realistische Analysen mit der Methode der gekoppelten Kanäle durchgeführt, wobei der  $1^+$ -Grundzustand sowohl mit dem  $3_1^+$ -Resonanzzustand als auch mit den beiden Kontinuums-Zuständen gekoppelt wird. Eine gleichzeitige Anpassung an die gemessenen differentiellen Wirkungsquerschnitte schränkt die Art und Stärke der Kopplung stark ein. Es wird aufgezeigt, daß die komplexen Kopplungsschematas von CDCC-Analysen unbedingt durch experimentelle Daten kontrolliert werden müssen um Fehldeutungen einzelner Ergebnisse zu vermeiden. In dem untersuchten Fall spielen Mehrstufenprozesse über virtuelle Zwischenzustände nur eine untergeordnete Rolle.

## 1. Introduction

The role of the continuum for the excitation of nuclei by scattering of nuclear particles is an issue of considerable interest, in view of the feedback to scattering from (quasi) discrete nuclear states as well as to final state interactions through (particle) continuum couplings (rescattering) of the fragments of the excited nucleus. A powerful theoretical tool to approach such questions is the Coupled Discretized Continuum Channels (CDCC) method [1]. Extensive analyses based on this method, have revealed a distinct influence of nuclear breakup of loosely bound projectiles (such as deuteron,  ${}^6, {}^7\text{Li}$  etc.) on elastic scattering from nuclei [2]. However, the practical procedures of CDCC analyses are usually affected and biased by the theoretical assumptions about the involved microscopic interaction and the structure model, i.e. about the formfactors specifying strength and radial distribution of the coupling. In particular, usually the continuum effects of the theoretical assumptions are ill-founded and withdraw experimental control. Thus, when exploring details of inelastic excitation or projectile breakup, in particular, when additionally an interference pattern of the nuclear and the long-range Coulomb interaction might be present, an increased sensitivity to the simplifications and constraints of the theoretical ingredients may lead to controversial results. The ambiguity that identical experimental cross section data can be alternatively reproduced on one hand with phenomenological formfactors and a relatively simple coupling scheme [3] and on the other hand, by use of microscopically constructed formfactors with a rather complex and delicate competition of higher order nuclear and Coulomb excitation paths [4], is still a matter of debate.

Especially, in the case of  ${}^6\text{Li}$  scattering and breakup, such irritating features - the dependencies on the theoretical input - (see also the analyses of 60-MeV  ${}^6\text{Li}$  scattering [5]) - have become conspicuous. Nevertheless,  ${}^6\text{Li}$  appears to be a good testing ground to look for continuum coupling effects. The first excited state ( $3_1^+$ ,  $E_x = 2.185$  MeV) is embedded as a narrow resonance in the ( $\alpha + d$ ) continuum, which starts with the  $\alpha + d$  threshold at 1.47 MeV above the  ${}^6\text{Li}$  ground state. This situation provides a convenient possibility to study effects of the nonresonant continuum excitation, just below and above the resonance. There, the low relative energies of  $\alpha + d$  fragments may enhance the rescattering probability, and it has been suggested [6, 7] that a *recombination* of the  $\alpha$ -particle and deuteron fragments may contribute as a real process to the small-angle decrease ( - usually interpreted as Coulomb excitation feature - ) of the breakup cross section below a critical value of the momentum transfer ( $p_{\text{crit}} \sim 117 \text{ MeV}/c$ ).

Such a suggestion arises from the observation of some inadequacies of one-step (DWIA and DWBA) calculations for proton and  $\alpha$ -particle induced  ${}^6\text{Li}$  breakup [6-9].

The present attempt to identify continuum coupling effects is based on analyses of observed elastic and inelastic scattering of protons and  $\alpha$ -particles from  ${}^6\text{Li}$  at projectile energies well above the Coulomb barrier. The angular range of the data covers the diffraction region, where the cross sections are dominated by the nuclear interaction. For the coupled channel analyses, using phenomenological formfactors with flexible radial shapes and adjusted strength parameters, the continuum above  $E_x=1.47$  MeV is discretized and various different couplings schemes are analyzed.

First results have been briefly communicated in ref. [10].

## 2. Experimental data

The analyses are based on measured differential cross sections of  ${}^6\text{Li}(\alpha, \alpha'){}^6\text{Li}$  and  ${}^6\text{Li}(p, p'){}^6\text{Li}$  scattering experiments, described with more details in refs. [6, 8].

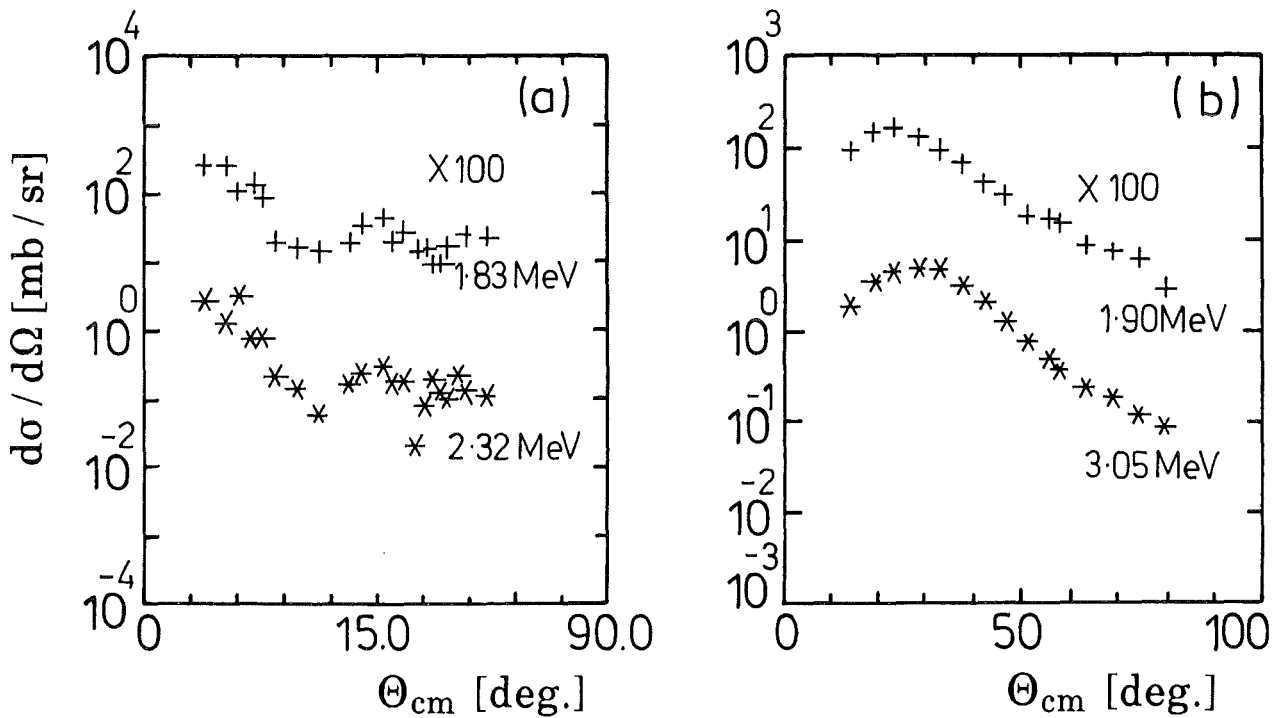


Fig. 1: Differential cross sections of the discretized continuum for 50-MeV  $\alpha$ -particle (a) and 65-MeV proton scattering (b) from  ${}^6\text{Li}$ .

From the  ${}^6\text{Li}(\alpha, \alpha')$  data at  $E_\alpha = 50$  MeV [8] we have extracted the continuum data by discretizing the (1.47-2.47 MeV) continuum into two bins (1.47-2.185 MeV) and (2.185-2.47 MeV) respectively. The angular distribution data of the corresponding centroid energies 1.83 MeV and 2.32 MeV are shown in Fig. 1. The  ${}^6\text{Li}(p, p')$  continuum data at  $E_p = 65$  MeV [6] extracted in (1.75-2.05 MeV) and (2.85-3.25 MeV) continuum bins are also shown in Fig. 1. The centroid energies are taken at 1.90 and 3.05 MeV respectively. Experimental cross sections for elastic and inelastic scattering from  $3_1^+$  state are displayed in Figs. 2 and 3 together with results of one-step DWBA calculations.

### 3. Coupled channel analyses

The analyses use the coupled-channel code ECIS 88 and various refinements of the (second order) "vibrational model" option provided there. It should be stressed (again) that the phenomenological coupling factors of the vibrational model type do not necessarily imply a collective excitation mode, since any (microscopically reasonable) formfactor resembles the "derivative" shape at the surface and can be approximated by an adequate choice of the shape and strength ("deformation") parameters. Thus the "vibrational model" choice, if flexibly handled, does not introduce a doubtful constraint for a phenomenological analysis of the coupling effects. For each excited state quadrupole excitation ( $\ell = 2$  transfer) is considered. As a reference for the coupled channel calculations, first the one-step DWBA cross sections (ignoring couplings through virtual excitations of intermediate states) are generated. These cross sections are shown in Figs. 2 and 3, normalized to the data. The corresponding optical potential parameters of the real and the imaginary part (volume and surface absorption) are given in Tab. 1, using conventional notation. The normalization factors (strengths of direct coupling) are given in Tab. 2. In the coupled channel calculations Coulomb excitation is included on equal footing by using a Coulomb "deformation" parameter  $\beta_c$ , scaled by the relation  $\beta_c R_c = \beta_v \cdot R_v$ ,  $R_c = r_c \cdot A^{1/3}$  being the (equivalent) charge radius of the nucleus and  $R_v$  the half-way radius of the (real) optical potential. This normalization is automatically done by the ECIS code ("heavy ion" option) during the calculation iterations.



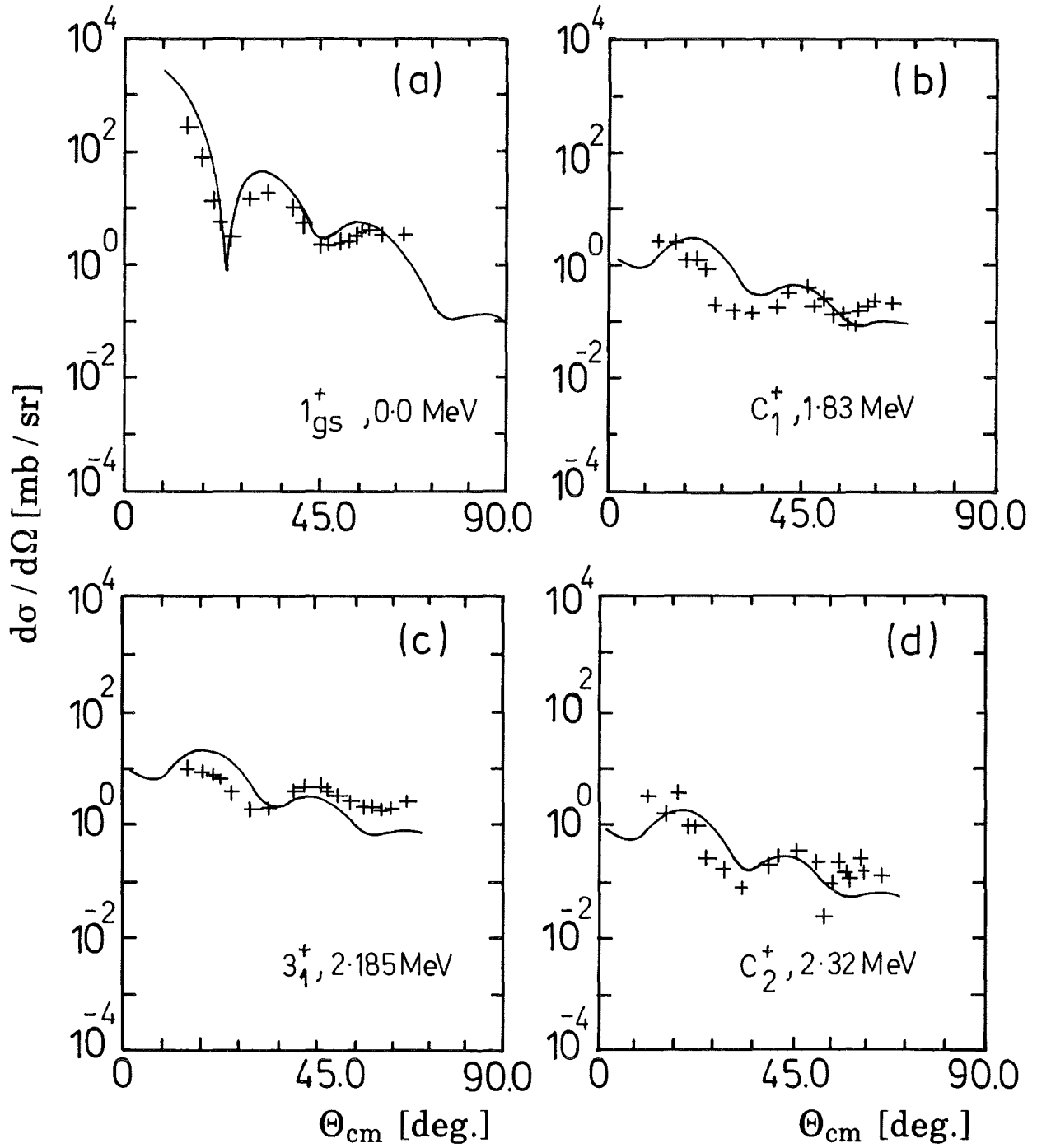


Fig. 2: Experimental  ${}^6\text{Li}(\alpha, \alpha'){}^6\text{Li}^*$  differential cross sections at  $E_\alpha=50 \text{ MeV}$  as compared to DWBA calculations.

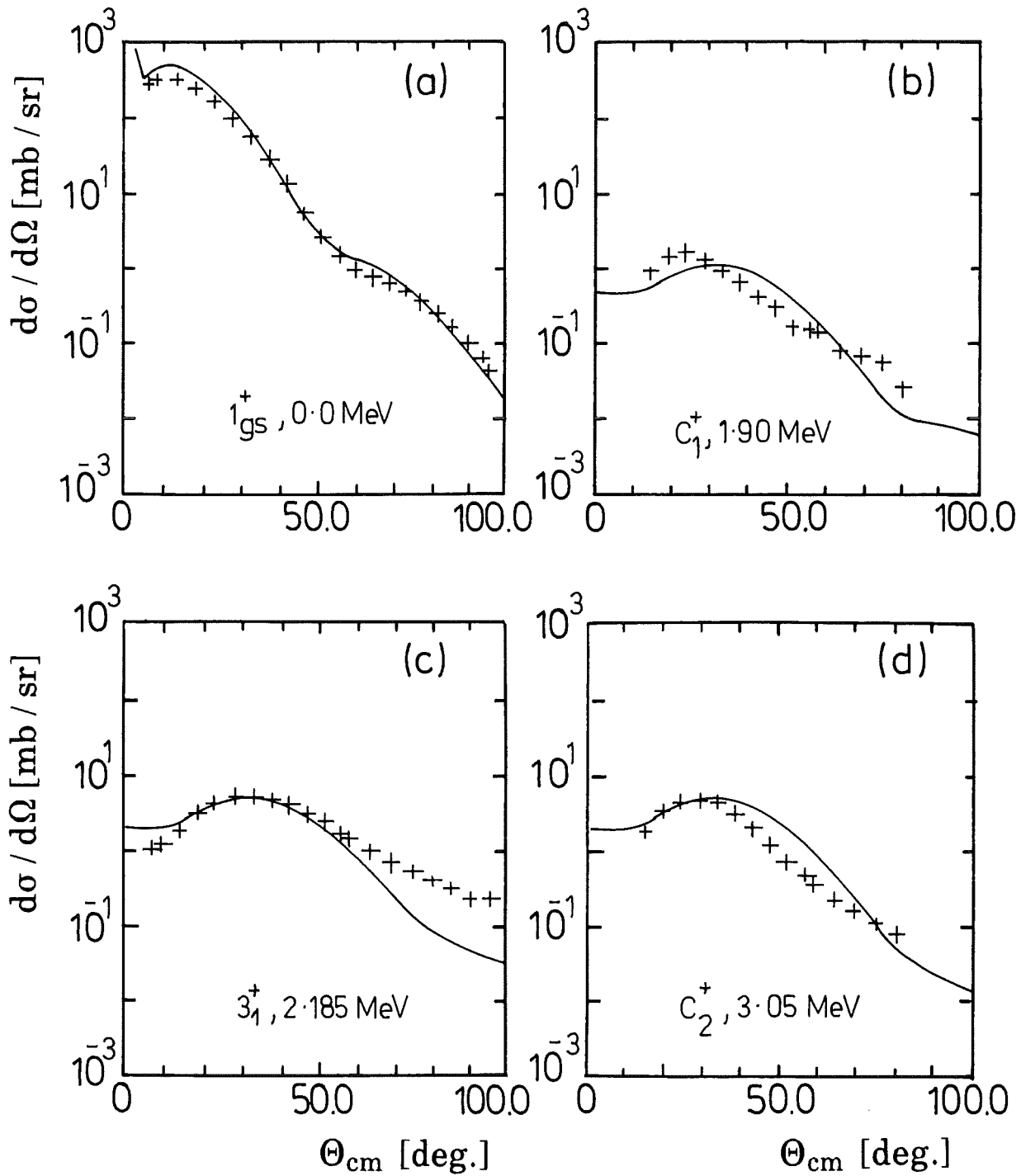


Fig. 3: Experimental  ${}^6\text{Li}(p, p'){}^6\text{Li}^*$  differential cross sections at  $E_p=65$  MeV as compared to DWBA calculations.

In the following we describe the results of coupled channel analyses with various coupling schemes of increasing complexity. The basic excitation paths are pictorially displayed in Fig. 4: One-phonon and two-phonon excitation modes.

Table 1: Optical potential parameters

	${}^6\text{Li} (\alpha, \alpha') {}^6\text{Li}$ $E_\alpha = 50 \text{ MeV}$ [8]	${}^6\text{Li} (p, p') {}^6\text{Li}$ $E_p = 65 \text{ MeV}$ [6]
$V_o$ [MeV]	85.98	36.74
$r_o$ [fm]	1.15	1.158
$a_o$ [fm]	0.80	0.757
$W_o$ [MeV]	0.0	3.89
$r_i$ [fm]	-	0.513
$a_i$ [fm]	-	0.875
$W_D$ [MeV]	14.01	3.615
$r_D$ [fm]	1.70	1.183
$a_D$ [fm]	0.657	0.543
$V_{so}$ [MeV]	-	4.815
$r_{so}$ [fm]	-	1.256
$a_{so}$ [fm]	-	0.705
$r_c$ [fm]	1.3	1.25

$$\begin{aligned}
 U(r) = & -V_o (1 + \exp((r-r_o \cdot A^{1/3})/a_o))^{-1} \\
 & -iW_o (1 + \exp((r-r_i \cdot A^{1/3})/a_i))^{-1} \\
 & -4iW_D \cdot a_D \frac{d}{dr} (1 + \exp((r-r_D \cdot A^{1/3})/a_D))^{-1} \\
 & + \left(\frac{\hbar}{m_n c}\right)^2 V_{so} \frac{1}{r} \frac{d}{dr} (1 + \exp((r-r_{so} \cdot A^{1/3})/a_{so}))^{-1} \cdot \sigma \cdot l \\
 & + V_C
 \end{aligned}$$

Table 2: Coupling strengths of different transitions

	${}^6\text{Li} (\alpha, \alpha') {}^6\text{Li}$ $E_\alpha = 50 \text{ MeV}$	${}^6\text{Li} (p, p') {}^6\text{Li}$ $E_p = 65 \text{ MeV}$
$1_1^+ \Rightarrow 3_1^+$	0.53	0.65
$1_1^+ \Rightarrow C_1^+$	0.19	0.30
$1_1^+ \Rightarrow C_2^+$	0.19	0.65

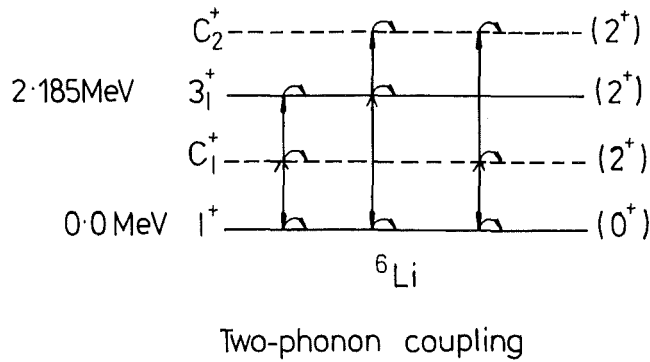
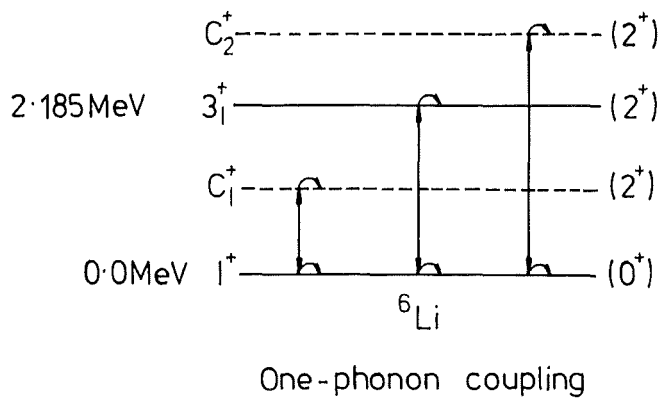


Fig.4: Coupling schemes of pure one-step and two-step quadrupole excitation modes including direct second-order and (diagonal) self-excitation [12].

a. One-step transitions

As compared to the first-order excitation by the DWBA mechanism the coupling (including the non-diagonal and diagonal second-order contributions [12]) does not significantly affect the theoretical cross sections, and the fits (Figs. 5 and 6) essentially restore the DWBA results (see also ref. 13).

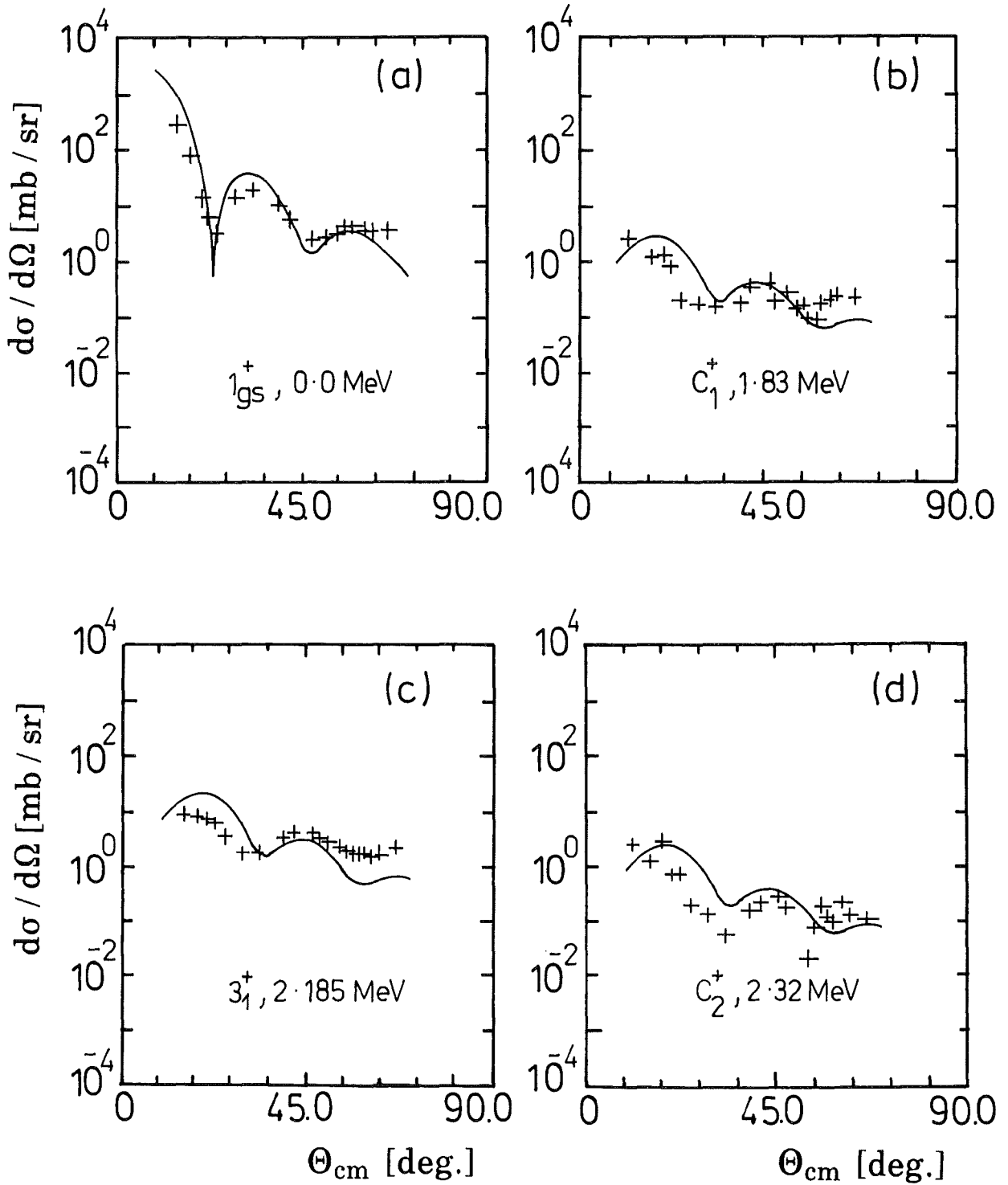


Fig. 5: Experimental differential cross sections of 50-MeV  $\alpha$ -particle scattering from  ${}^6\text{Li}$  as compared to coupled channels calculations in a  $1_{gs}^+ \Rightarrow C_2^+ \Rightarrow 3_1^+ \Rightarrow C_2$  one-step excitation scheme (Fig. 4).

b. Two-step transitions

Fig. 7 indicates various coupling schemes involving two-step excitation modes.

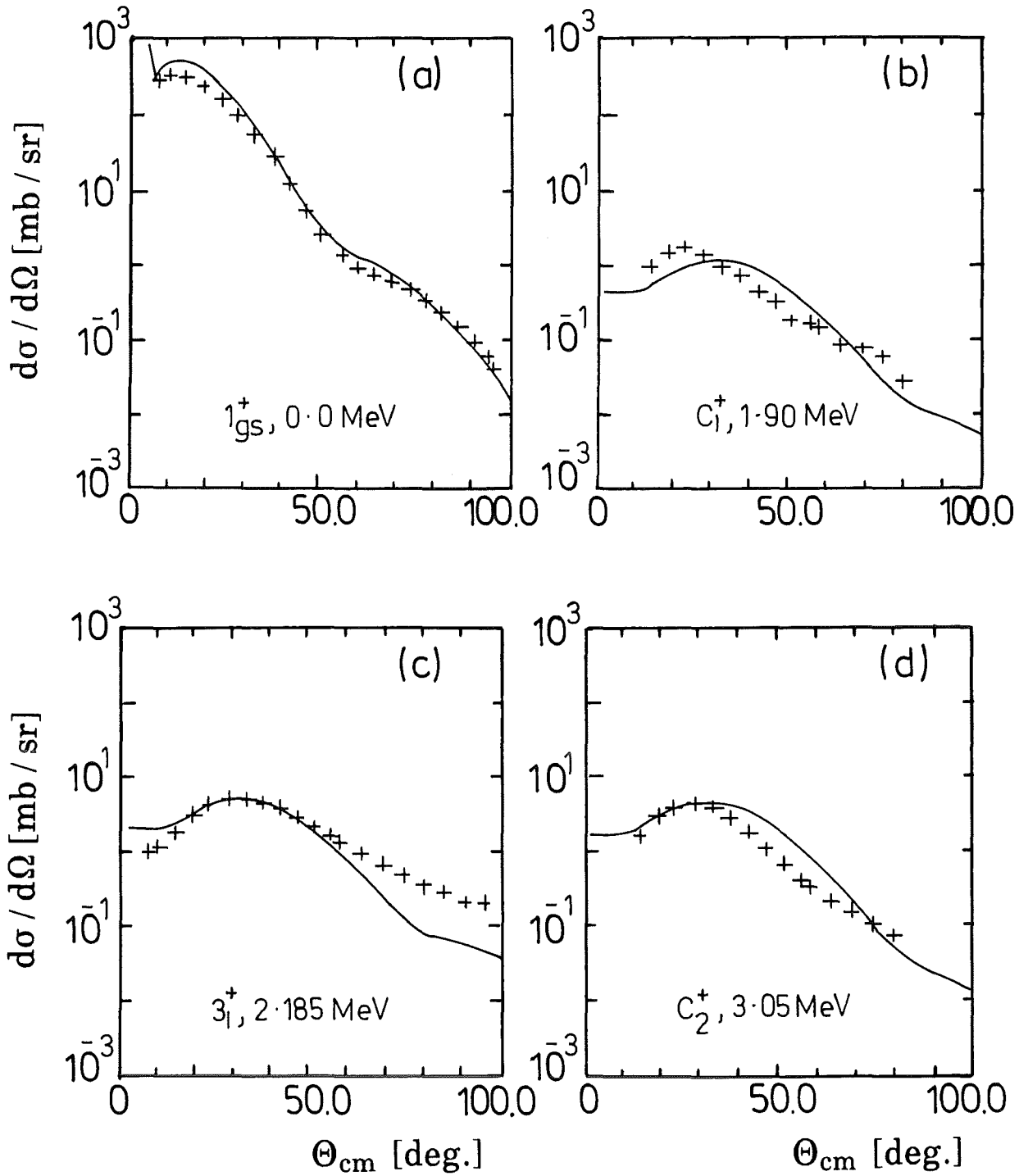


Fig. 6: Experimental differential cross sections of 65-MeV proton scattering from  ${}^6\text{Li}$  as compared to coupled channels calculation in a  $1_{gs}^+ \Rightarrow C_2^+ \Rightarrow 3_1^+ \Rightarrow C_2^+$ -one-step excitation scheme (Fig. 4).

These schemes adopt a pure "two-phonon" structure of one of the involved states, and this constraint, enforcing two-step excitations, affects significantly magnitudes and shapes of the cross sections. In general, a search for the optimum values of the  $\beta$ -parameters (together with varying the imaginary potential) has

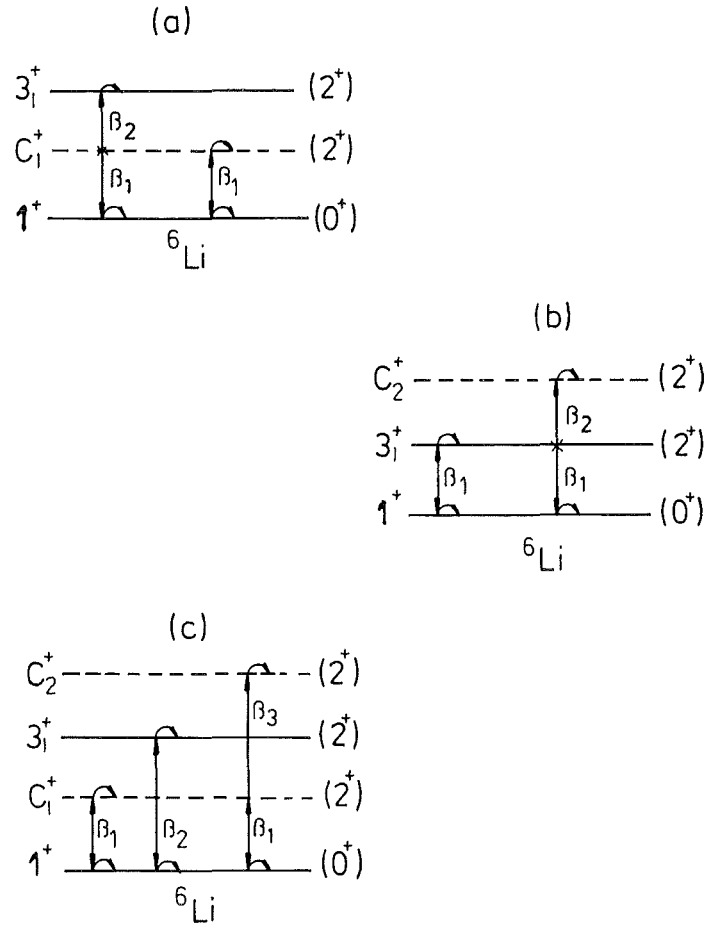


Fig. 7: Various studied coupling schemes with two-step excitation modes.

been performed. It turns out that the best fits lead to rather modest descriptions of the data, especially for the adopted "two-phonon" states the cross sections are drastically underestimated, even with unreasonably large values of the corresponding deformation parameters.

Fig. 8 displays this feature for a pure two-step excitation of the  $3_1^+$  resonance by 50-MeV  $\alpha$ -particle scattering.

The features are similar in the case of proton scattering. An example is shown in Fig. 9.

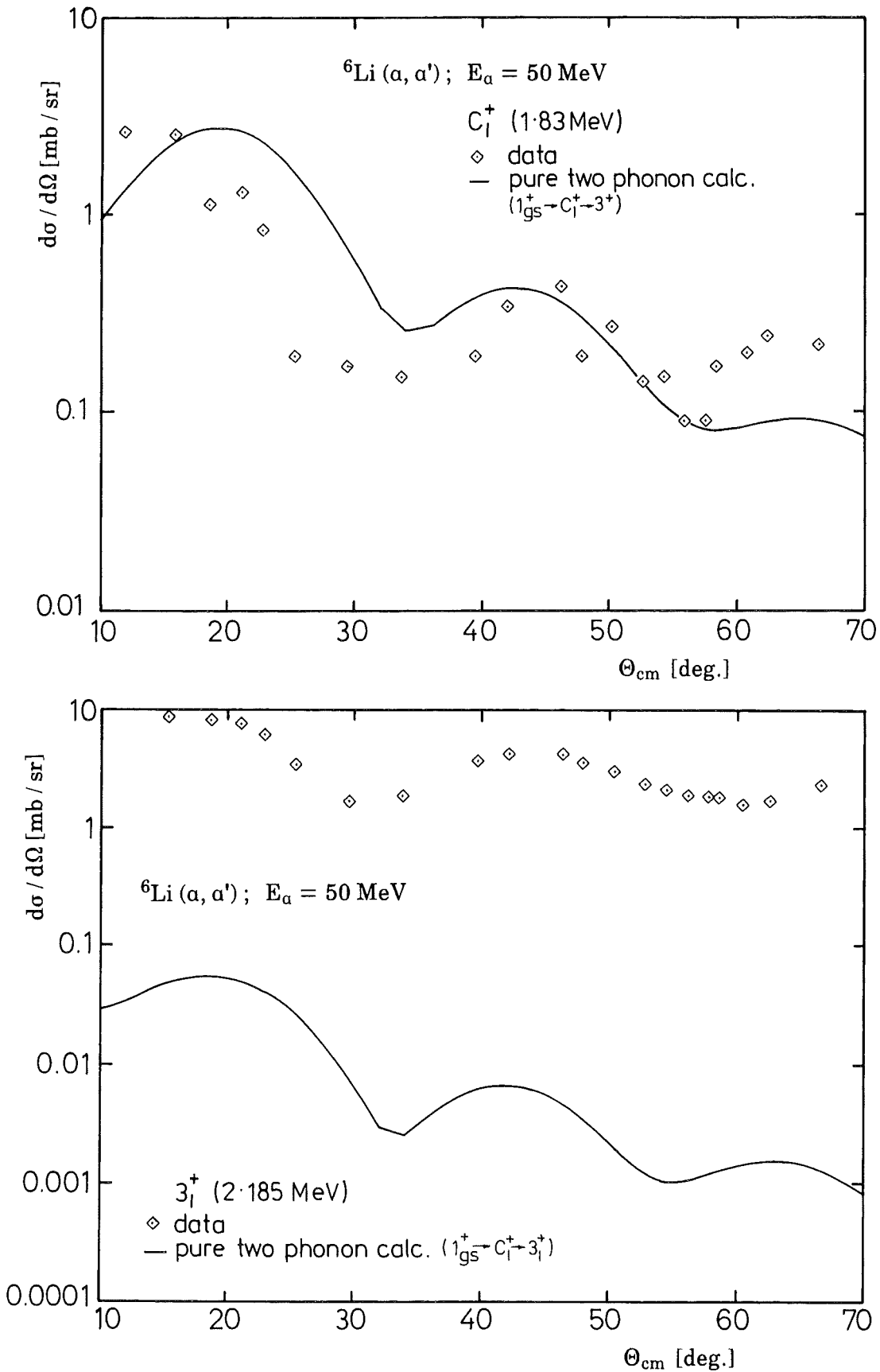


Fig. 8: Results of the  $1_{\text{gs}}^+ \Rightarrow C_1^+ \Rightarrow 3_1^+$ -two-step excitation by 50-MeV  $\alpha$ -particle scattering, showing the minor contribution of two-step transition to the  $3_1^+$  resonance.



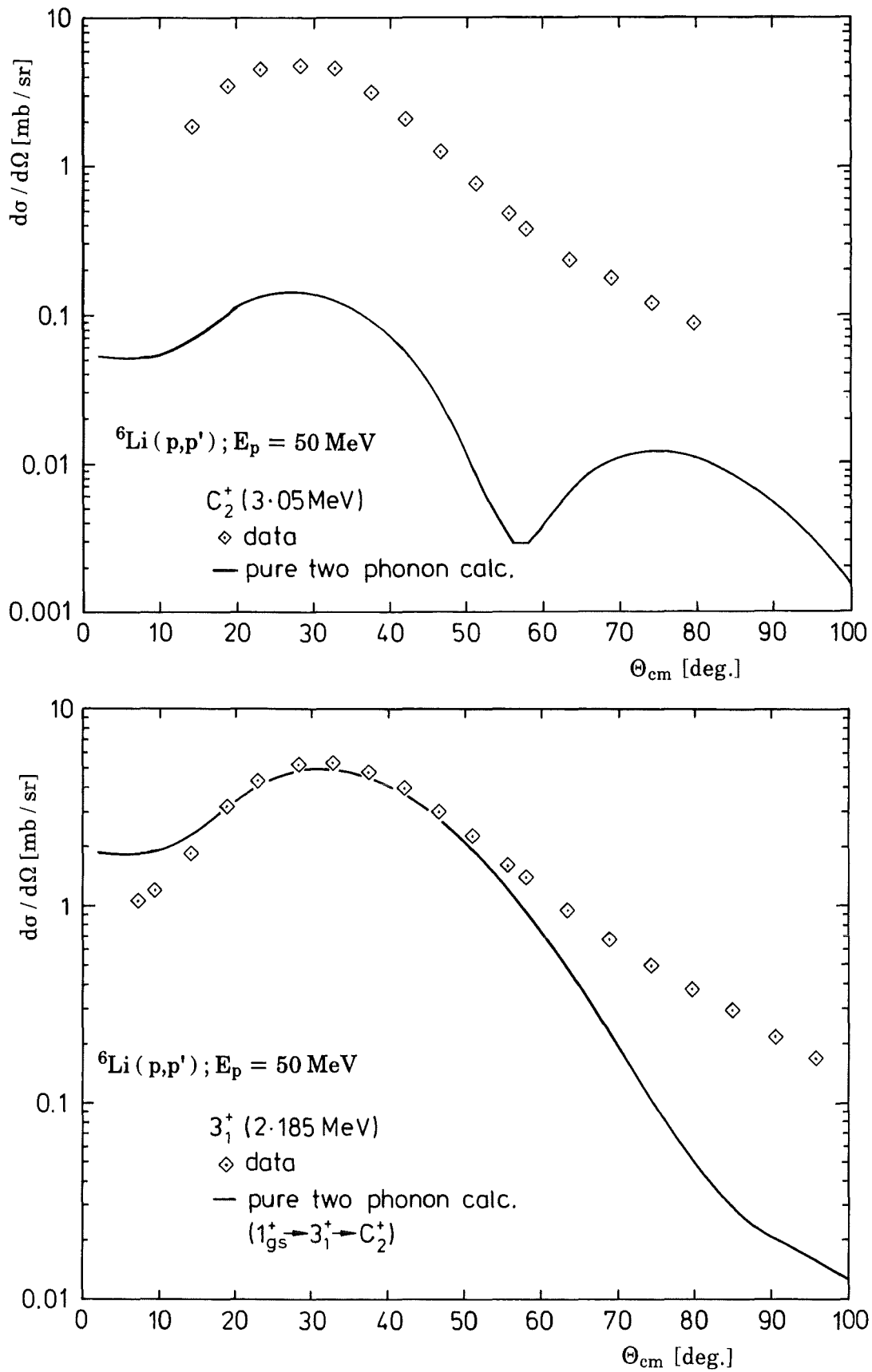


Fig. 9: Results of the  $1_{gs}^+ \Rightarrow 3_1^+ \Rightarrow C_2^+$ -two-phonon excitation by 65-MeV proton scattering, indicating the minor contribution of two-step transitions to the continuum state  $C_2^+$ .

c. Competition of one-step and two-step processes

In order to enable simultaneous excitations by one-step and two-step processes, in the frame work of the vibrational model (which is actually used in a rather anharmonic version) the involved states have to be specified as a mixture of one-phonon (1 ph) and two-phonon (2 ph) amplitudes

$$|I; 1 ph + 2 ph \rangle = \cos \alpha |1 ph \rangle + \sin \alpha |2 ph \rangle$$

defined by the mixing angle  $\alpha$ .

The studied coupling schemes are indicated in Fig. 10.

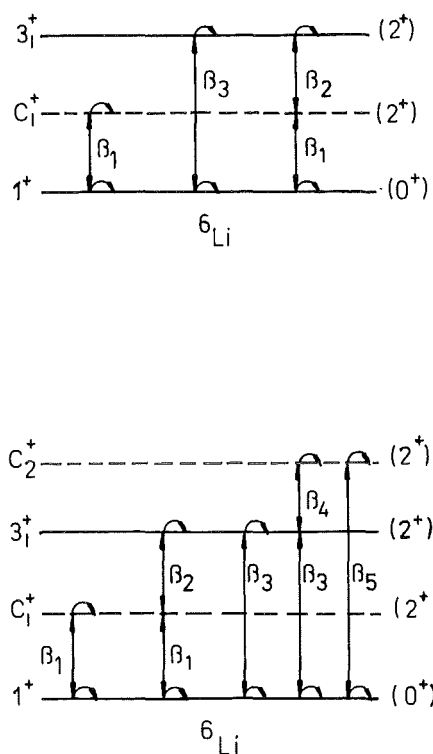


Fig.10: Coupling schemes indicating competing amplitudes for one-step and two-step excitation.

Varying the mixing angle  $\alpha$  (together with other parameters), the optimum value for  $\alpha$  ( $3_1^+$ ) =  $40^\circ$  is found reproducing  $\alpha$ -particle scattering from the  $3_1^+$  state as displayed in Fig. 11. As a typical feature for the interference of one-phonon and two-phonon excitation amplitudes, the calculated cross section exhibits a steeper slope with increasing scattering angle. In contrast, this feature is less pronounced in the one-step approach, which prefers a more global fit to the data (see Fig. 5).

The calculations have been extended to the scheme shown in Fig. 10b, allowing additionally the presence of one-step and two-step amplitudes for the excitation of the continuum state  $C_2^+$ . Again the effect of two-step excitation appears to be

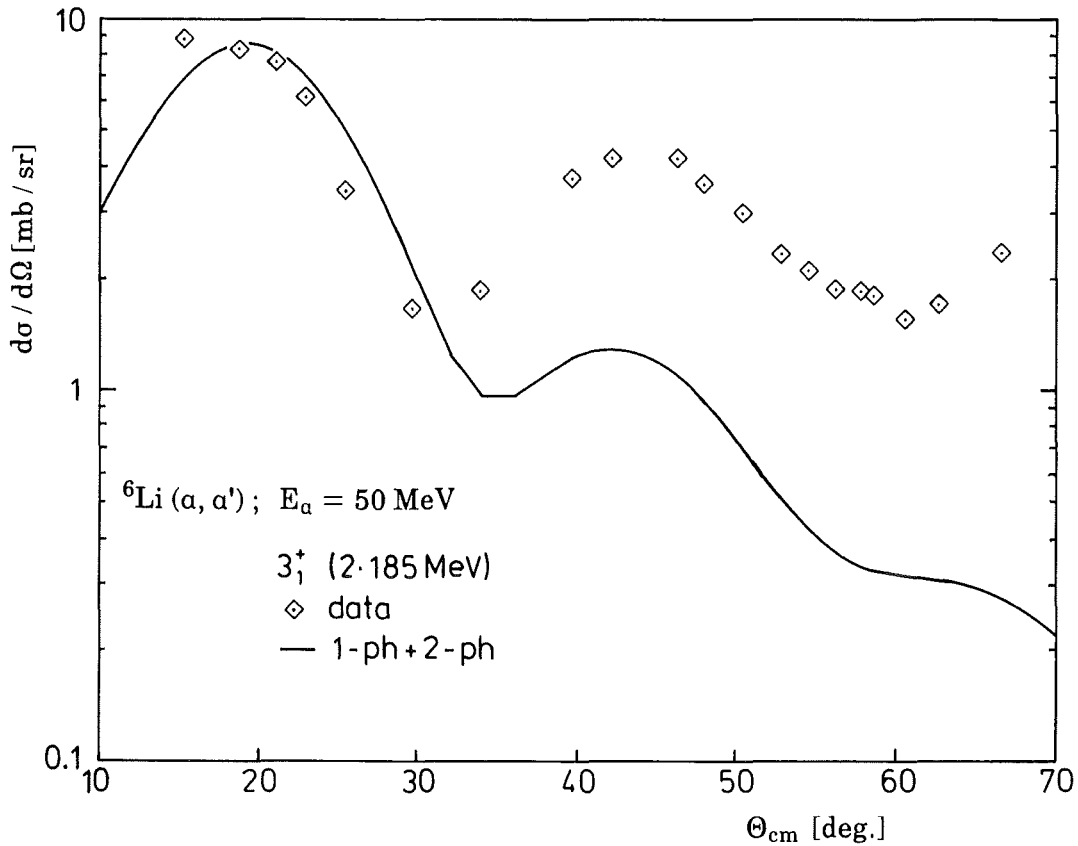


Fig.11: The theoretical differential cross section for the  $3_1^+$  excitation in  ${}^6\text{Li}$  by 50-MeV  $\alpha$ -particle scattering, calculated in  $1_{gs}^+ \Rightarrow C_1^+ - 3_1^+$  coupling scheme with interfering one- and two-step processes (see Fig. 10).

insignificant, and large two-step amplitudes result in a considerable under-prediction of the cross sections.

Thus, we arrive at the conclusion that the coupling effect through higher-order processes is negligible compared to the one-step-excitation, which is already well described by the DWBA approach. The minor importance of multistep processes inferred from the data appears quite conclusive, as the calculations prove to be rather sensitive to the coupling strengths and coupling modes. Arbitrary variations of the coupling strengths effect distinctly magnitudes and shapes of the calculated inelastic scattering cross sections, while the optical potential parameters are essentially defined by elastic scattering.

All calculations have been performed for  ${}^6\text{Li}(\alpha, \alpha') {}^6\text{Li}$  as well as for the  ${}^6\text{Li}(p, p') {}^6\text{Li}$  scattering. The proton scattering case exhibits the same features and confirms the general conclusions about the absence of a significant channel-coupling of  $3_1^+$  resonance and the low lying continuum states in  ${}^6\text{Li}$ .

#### 4. Concluding remarks

As a possible explanation of a striking discrepancy of results of three-body-final-state DWIA calculations [9] with the experimentally observed excitation of  ${}^6\text{Li} \Rightarrow \alpha + d$  breakup continuum by 50-MeV  $\alpha$ -particle and 65-MeV proton scattering, multistep excitation paths and coupling effects through the discretized continuum near the  $3_1^+$  resonance state of  ${}^6\text{Li}$  are investigated. The studies are performed in the spirit of the CDCC method which has been proven to be rather successful in explaining various anomalies of the  ${}^6\text{Li}$  scattering from nuclei [2]. The results allow following statements:

- Continuum coupling effects are minimal, and higher-order (multistep) processes through the nonresonant continuum contribute insignificantly to the nonresonant and resonant breakup, induced by nuclear scattering.
- The calculated cross sections are rather sensitive to the coupling modes, and any artificial enhancement or arbitrary variation of the coupling strengths destroys the agreement of the calculations with the experimental data.
- In turn, due to the complexity of the CDCC coupling schemes, invoking intermediate (discretized) continuum states, CDCC analyses need the control by experimental data for the involved states, in order to avoid artefacts in interpreting a particularly selected data set.

*The authors gratefully acknowledge helpful discussions with Dr. Subnit Roy. We are grateful to Dr. M. Fujiwara and Dr. M. Tosaki for providing us the  ${}^6\text{Li}(p,p')$  data in a tabulated form. One of us (H.R.) thanks the Saha Institute of Nuclear Physics, Calcutta, for the hospitality during a short research visit, when the idea of the described studies has been borne out.*

## References

1. N. Austern and M. Kawai, *Progr. Theoret. Phys.* **80**, 694 (1988)
2. Y. Sakuragi, M. Yahiro and M. Kamimura, *Progr. Theoret. Phys.* **89**, 136(1986)
3. J. Kiener, G. Gsottschneider, H.J. Gils, H. Rebel, V. Corcalciuc, S.K. Basu, G. Baur and J. Raynal, *Z. Phys. A* **339**, 489 (1991)  
see G. Baur and H. Rebel, *J. Phys. G : Nucl. Phys.* **20**, 1 (1994)
4. Y. Hirabayashi and Y. Sakuragi, *Phys. Rev. Lett.* **69**, 1892 (1992)
5. K. Rusek, N. M. Clarke and R.P. Ward, *Phys. Rev.* **C50**, 2010 (1994)
6. M. Tosaki, M. Fujiwara, K. Hosono, T. Noro, H. Ito, T. Yamazaki and H. Ikegami, *Nucl. Phys.* **A493**, 1 (1989) - M. Tosaki, private communication
7. C. Samanta, T. Sinha, Sudip Gosh, S. Ray and S.R. Banerjee, *Phys. Rev.* **C50**, 1226 (1994)
8. C. Samanta, Sudip Gosh, M. Lahiri, S. Ray and S.R. Banerjee, *Phys. Rev.* **C45**, 1757 (1992)
9. C. Samanta, M. Lahiri, Subnit Roy, S. Ray and S.R. Banerjee, *Phys. Rev.* **C47**, 1313 (1993)
10. Rituparna Kanungo, M. Lahiri, C. Samanta and H. Rebel, *Z. Phys.* **A351**, 9 (1995)
11. J. Raynal, *Phys. Rev.* **C23**, 2571 (1981)
12. T. Tamura, *Rev. Mod.* **37**, 679 (1965)
13. Rituparna Kanungo, C. Samanta, Subnit Roy and S.K. Samadar, *Nucl. Phys.* **A581**, 294 (1995)

## Appendix: Results of coupled channel analyses

In this appendix we display additional results of coupled-channel analyses based on the schemes indicated in Fig. 4, 7 and 10.

Fig. A1 50-MeV  $\alpha$ -particle scattering from  ${}^6\text{Li}$ :

$1_{\text{gs}}^+ \Rightarrow 3_1^+$  direct ("one-phonon") coupling.

Fig. A2 65-MeV proton scattering from  ${}^6\text{Li}$ :

$1_{\text{gs}}^+ \Rightarrow 3_1^+$  direct ("one-phonon") coupling.

Fig. A3 50-MeV  $\alpha$ -particle scattering from  ${}^6\text{Li}$ :

$1_{\text{gs}}^+ \Rightarrow C_1^+ \Rightarrow 3_1^+$  direct ("one-phonon") coupling.

Fig. A4 65-MeV proton scattering from  ${}^6\text{Li}$ :

$1_{\text{gs}}^+ \Rightarrow C_1^+ \Rightarrow 3_1^+$  direct ("one-phonon") coupling.

Fig. A5 50-MeV  $\alpha$ -particle scattering from  ${}^6\text{Li}$ :

$1_{\text{gs}}^+ \Rightarrow C_1^+ \Rightarrow 3_1^+ \Rightarrow C_2^+$  direct ("one-phonon") coupling

with one- and two-step excitation processes for the  $3_1^+$  and  $C_2^+$  states.

Fig. A6 65-MeV proton scattering from  ${}^6\text{Li}$ :

$1_{\text{gs}}^+ \Rightarrow C_1^+ \Rightarrow 3_1^+ \Rightarrow C_2^+$  direct ("one-phonon") coupling

with one- and two-step excitation processes for the  $3_1^+$  and  $C_2^+$  states.

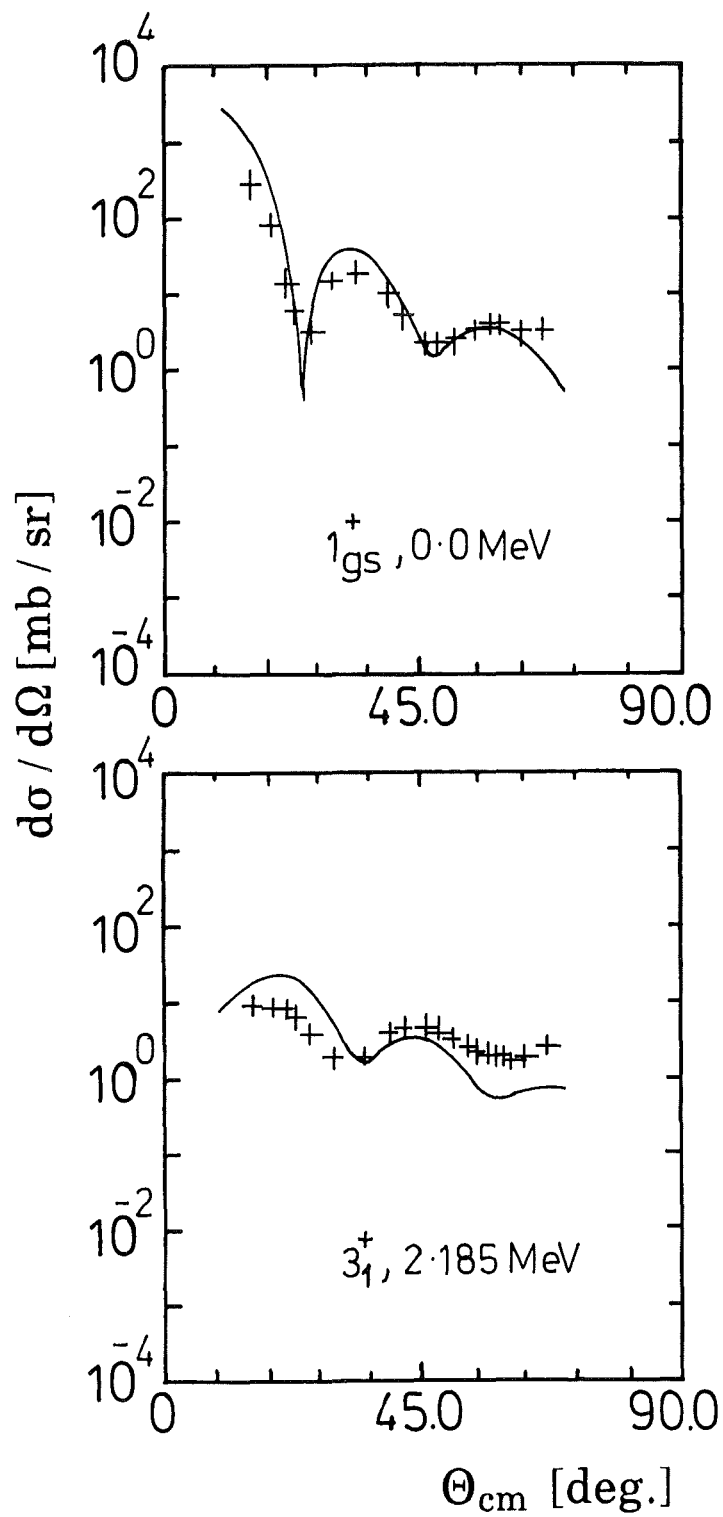


Fig. A1

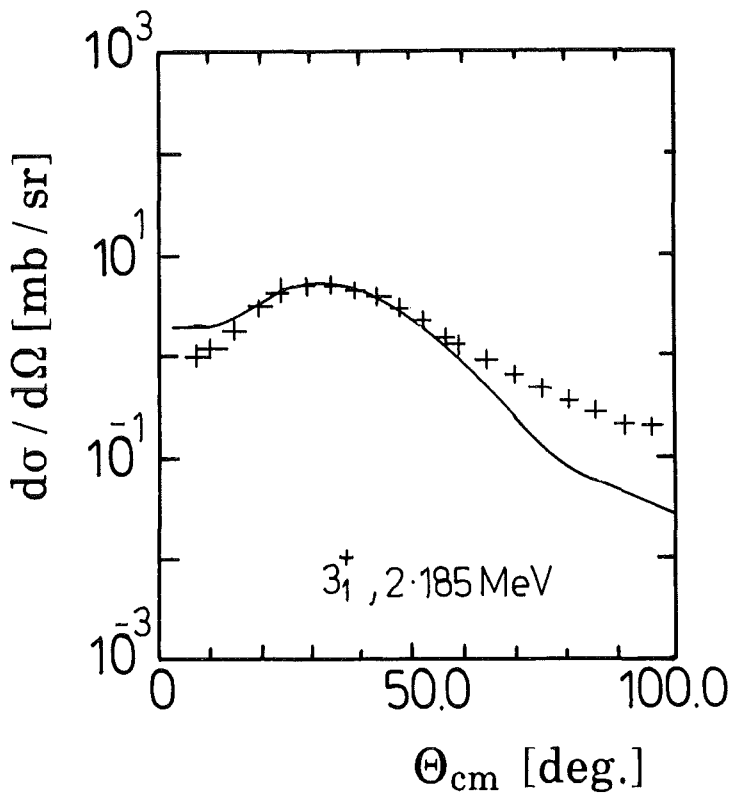
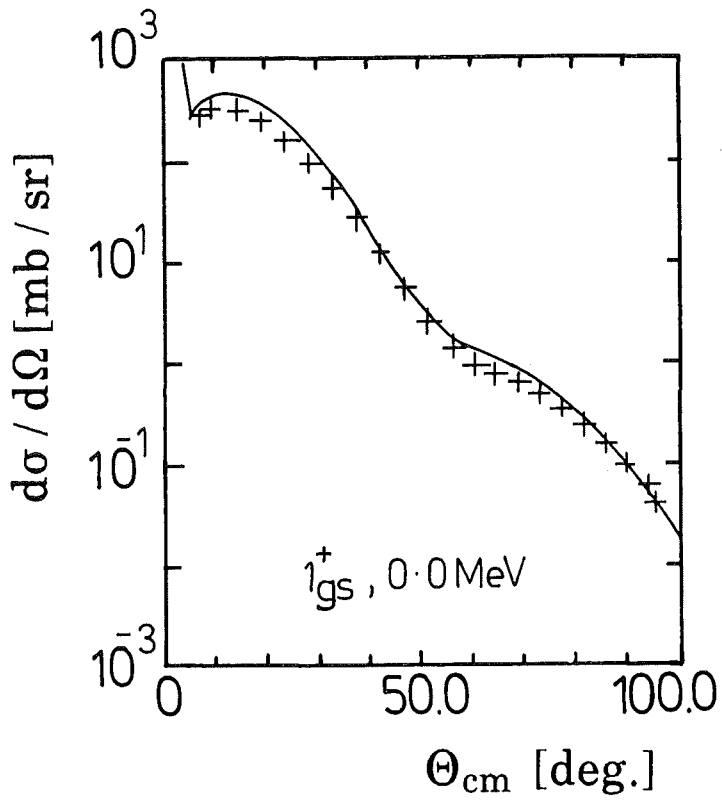


Fig. A2



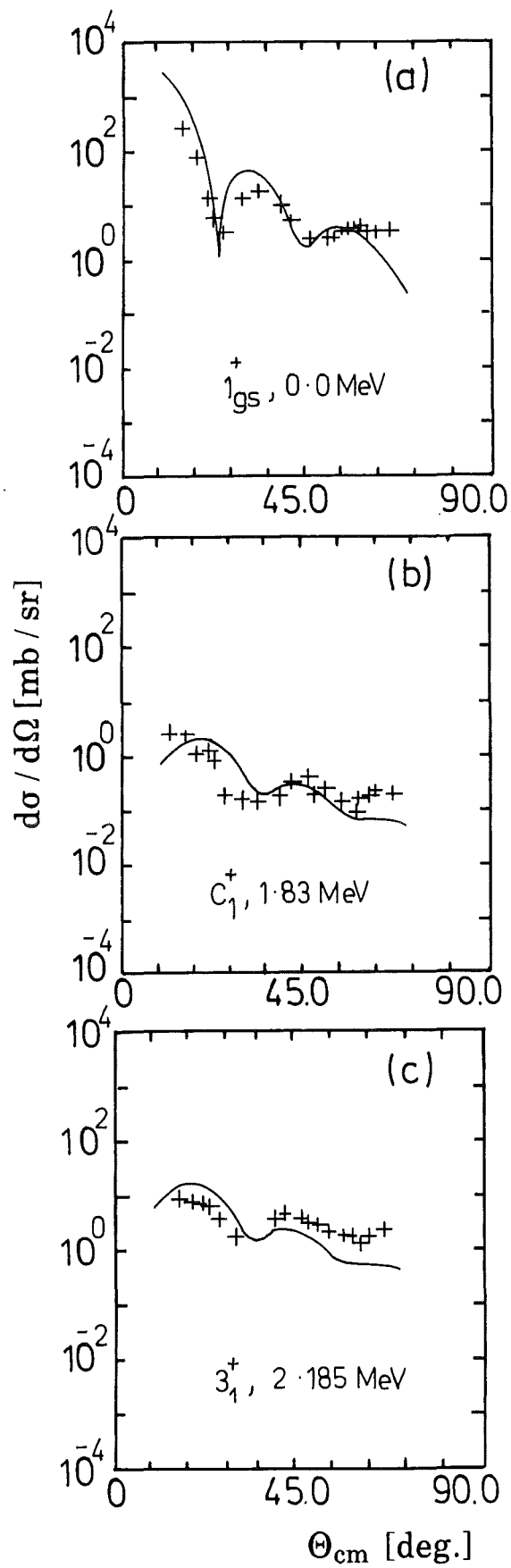


Fig. A3

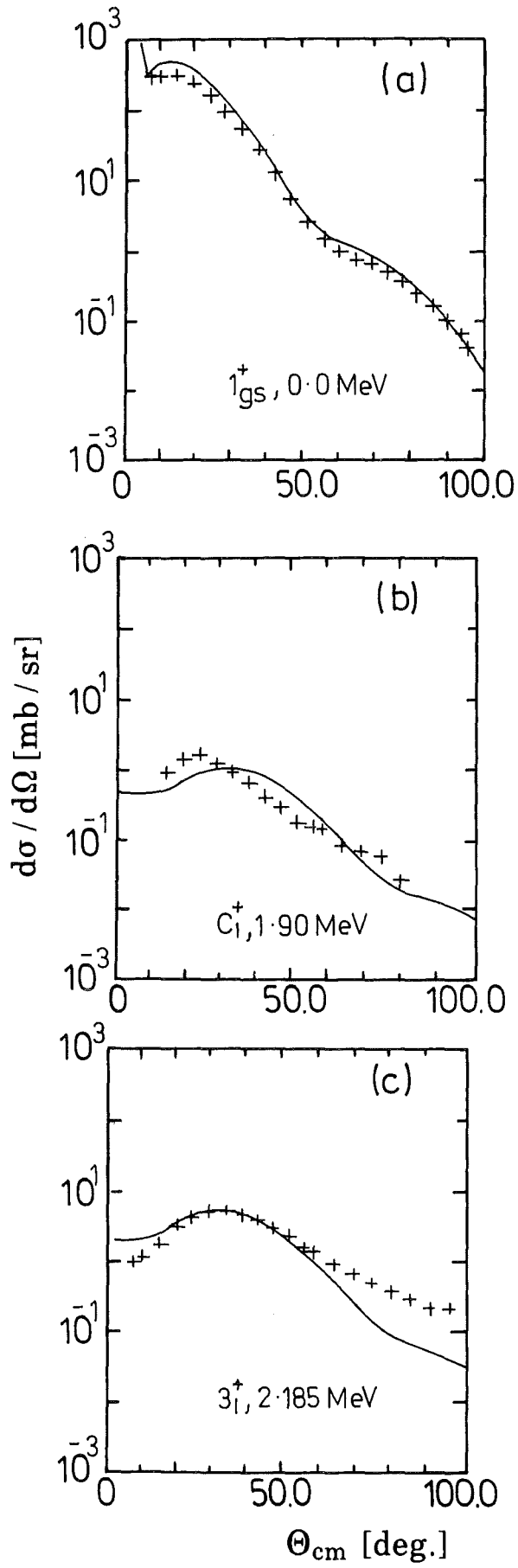


Fig. A4

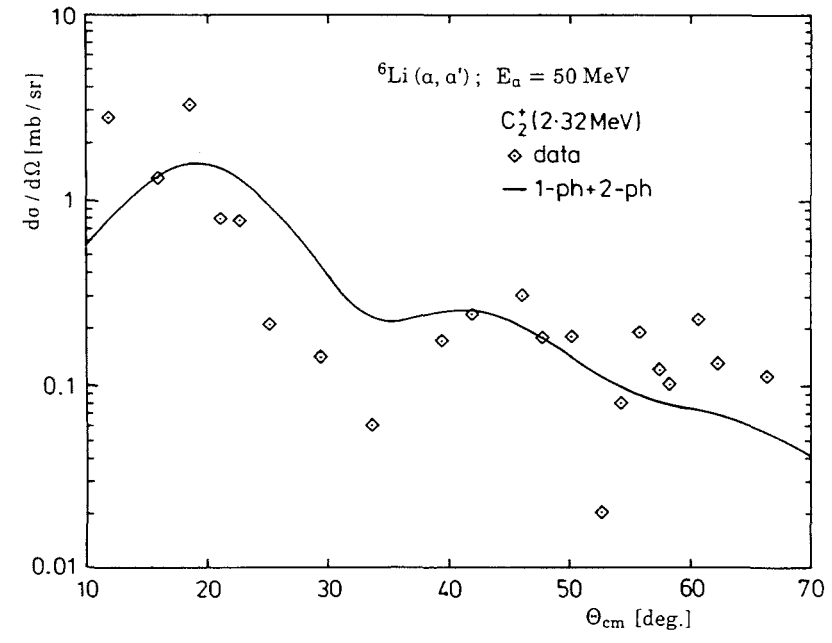
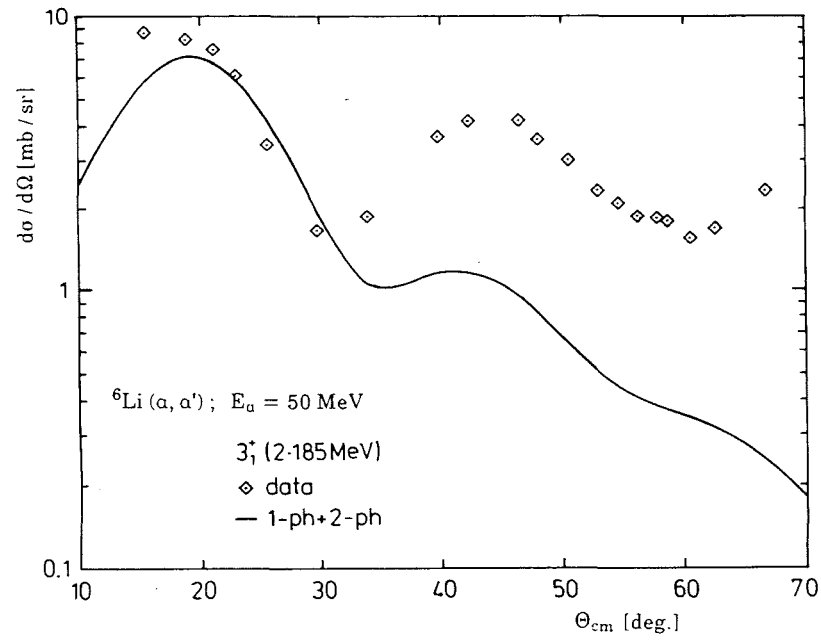
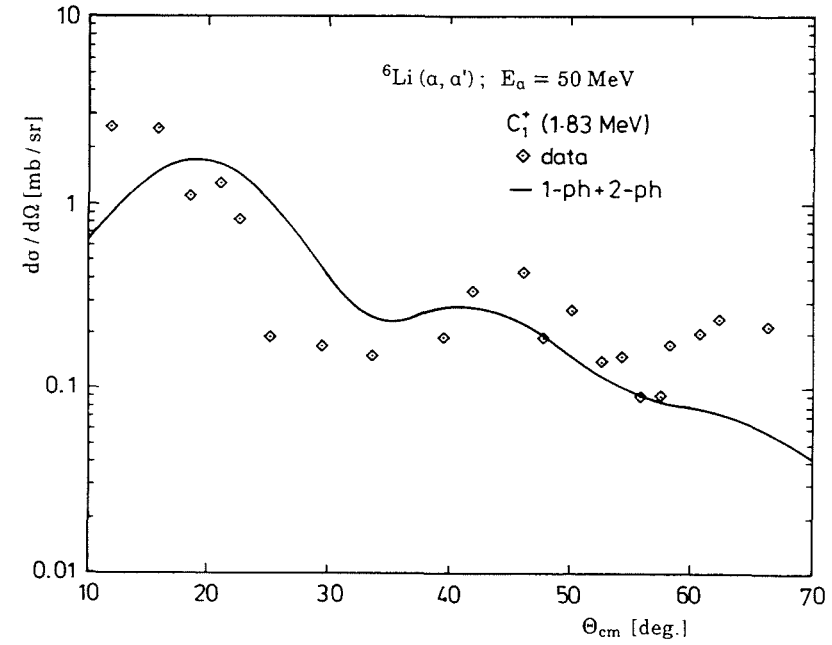
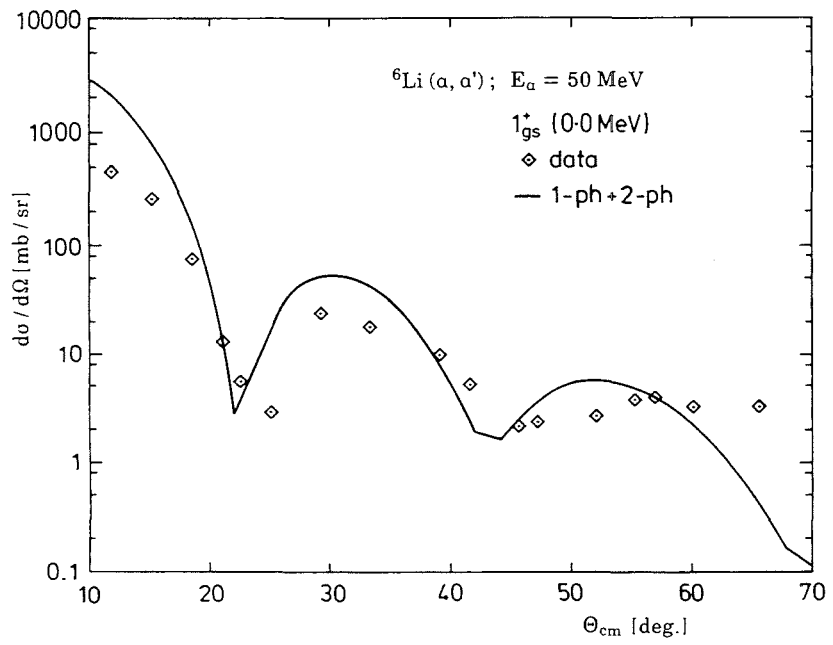


Fig. A5

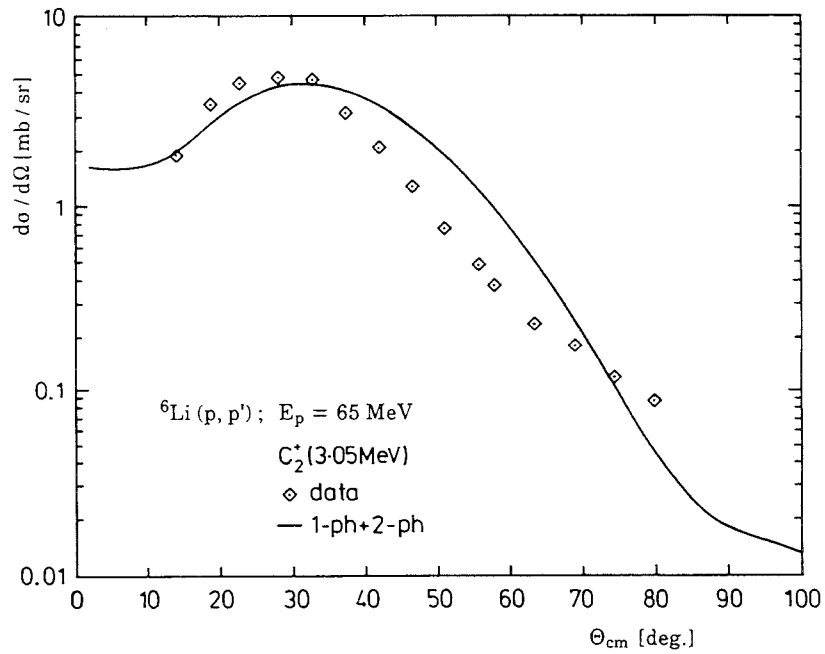
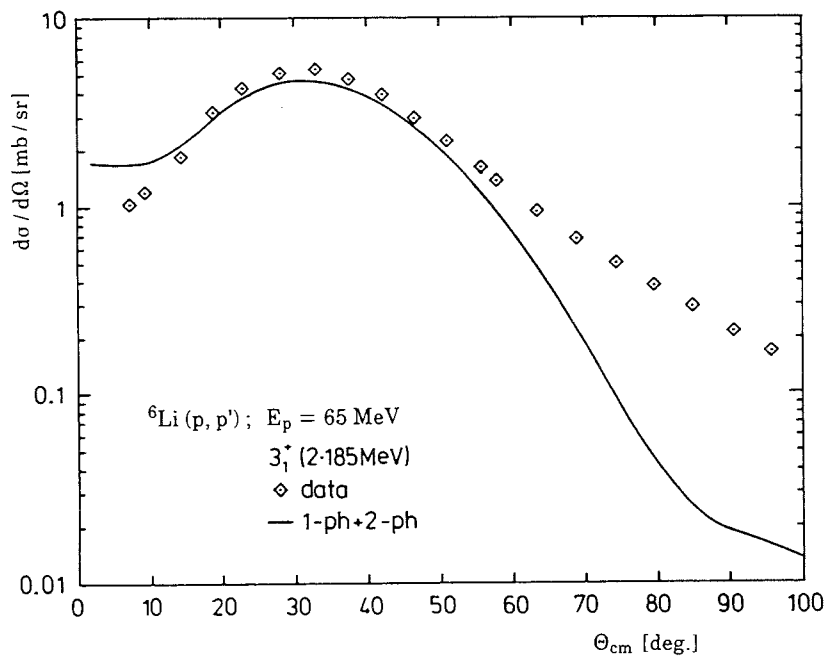
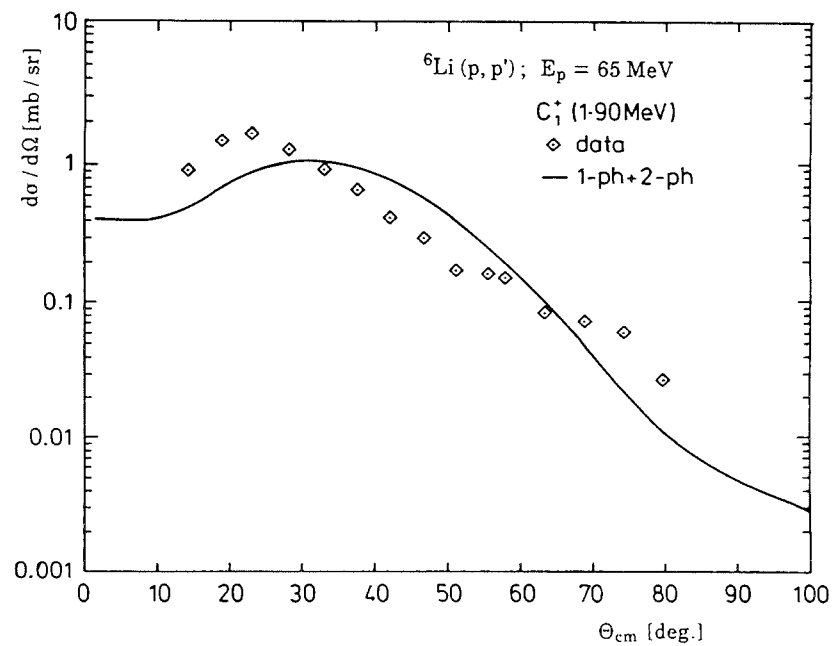
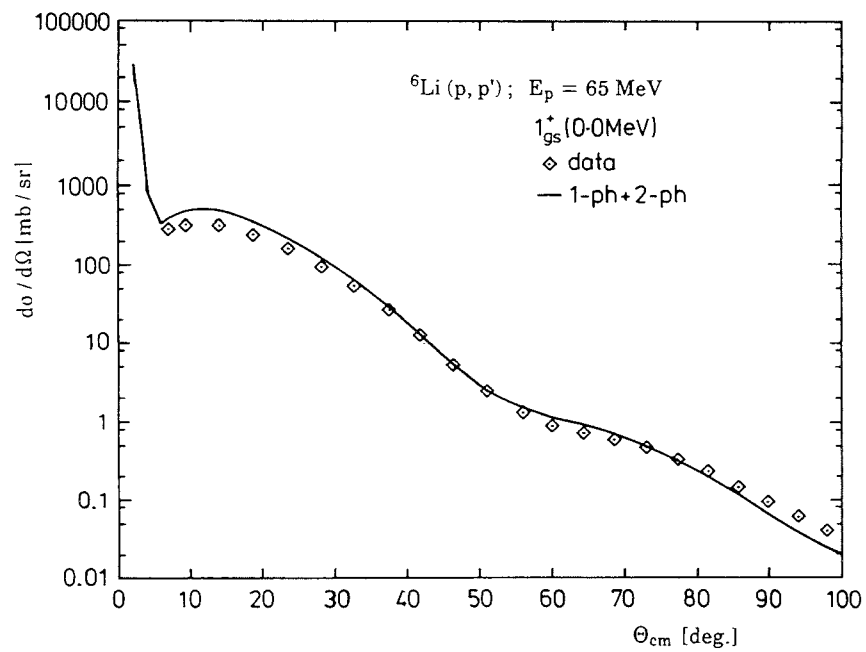


Fig. A6